

Effects of high octane additivated gasoline fuel on Three Way Catalysts performance under an accelerated catalyst ageing procedure

Herreros, J.M.; Oliva, F.; Zeraati-Rezaei, S.; Tsolakis, A.; Delgado, J.

DOI:

[10.1016/j.fuel.2021.122970](https://doi.org/10.1016/j.fuel.2021.122970)

License:

Creative Commons: Attribution-NonCommercial-NoDerivs (CC BY-NC-ND)

Document Version

Peer reviewed version

Citation for published version (Harvard):

Herreros, JM, Oliva, F, Zeraati-Rezaei, S, Tsolakis, A & Delgado, J 2022, 'Effects of high octane additivated gasoline fuel on Three Way Catalysts performance under an accelerated catalyst ageing procedure', *Fuel*, vol. 312, 122970. <https://doi.org/10.1016/j.fuel.2021.122970>

[Link to publication on Research at Birmingham portal](#)

General rights

Unless a licence is specified above, all rights (including copyright and moral rights) in this document are retained by the authors and/or the copyright holders. The express permission of the copyright holder must be obtained for any use of this material other than for purposes permitted by law.

- Users may freely distribute the URL that is used to identify this publication.
- Users may download and/or print one copy of the publication from the University of Birmingham research portal for the purpose of private study or non-commercial research.
- User may use extracts from the document in line with the concept of 'fair dealing' under the Copyright, Designs and Patents Act 1988 (?)
- Users may not further distribute the material nor use it for the purposes of commercial gain.

Where a licence is displayed above, please note the terms and conditions of the licence govern your use of this document.

When citing, please reference the published version.

Take down policy

While the University of Birmingham exercises care and attention in making items available there are rare occasions when an item has been uploaded in error or has been deemed to be commercially or otherwise sensitive.

If you believe that this is the case for this document, please contact UBIRA@lists.bham.ac.uk providing details and we will remove access to the work immediately and investigate.

1 **Effects of high octane additivated gasoline fuel on Three Way Catalysts**

2 **performance under an accelerated catalyst ageing procedure**

3 J.M. Herreros^{*a}, F. Oliva^b, S. Zeraati-Rezaei^a, A. Tsolakis^a, J. Delgado^b

4 *^aDepartment of Mechanical Engineering, School of Engineering, University of Birmingham, B15 2TT*
5 *Birmingham, UK*

6 *^bRepsol Technology Laboratory, Repsol, S.A. Calle Agustin Betancourt s/n, Mostoles, 28935, Spain*

7 *Corresponding author: JM Herreros. University of Birmingham, B15 2TT Birmingham, UK. J.herreros@bham.ac.uk

8 **Abstract**

9 The adoption of high octane rating fuels in Gasoline Direct Injection (GDI) engines helps to improve
10 fuel economy and thus reduce CO₂ emission. However, there is scarce literature regarding the impact
11 of additives used in high octane rating fuels on the performance and durability of the exhaust
12 aftertreatment components. This work investigates the effects of using an aniline (aromatic amine)
13 octane enhancer added to a commercial gasoline fuel on the activity of a commercial Three Way
14 Catalytic Converter (TWC) coupled to a GDI engine. TWC's capability in abating gaseous and particle
15 emissions is studied for both the additivated and the baseline fuel during and after a fuel-induced
16 accelerated catalyst ageing procedure. The accelerated catalyst ageing procedure is developed aiming
17 to identify the impact of the engine fuel on the catalyst poisoning, while limiting catalyst thermal
18 deactivation.

19 CO and NO conversion efficiencies in the TWC were close to 100% under the steady-state and transient
20 stoichiometric engine operation for both fuels during and after the catalyst ageing procedure. There was
21 a minor decrease (generally <10%) in the catalytic conversion efficiency of total HC for the additivated
22 fuel, but not being significant to reflect any TWC chemical deactivation. The aniline type octane
23 enhancer additive did not produce any detrimental effect on the TWC efficiency/performance. This
24 investigation demonstrates that fuels being designed to promote a more efficient GDI engine operation
25 can also enable the reduction of vehicle tailpipe CO₂ and pollutant emissions through synergies with
26 the TWC for cleaner road vehicles.

27 **Keywords:** fuel; three way catalyst; catalyst ageing; gaseous emissions; particulate matter; aromatic
28 amines

29 Nomenclature

- | | | | |
|----|---|----|---|
| 30 | aTWC: after Three Way Catalyst | 47 | GHG: Greenhouse Gases |
| 31 | BEVs: Battery Electric Vehicles | 48 | GHSV: Gas Hourly Space Velocity |
| 32 | bTWC: before Three Way Catalyst | 49 | ICE: Internal Combustion Engines |
| 33 | CAD: Crank Angle Degrees | 50 | IMEP: Indicated mean effective pressure |
| 34 | CO: Carbon Monoxide | 51 | MON: Motor Octane Number |
| 35 | COV: Coefficient Of Variation | 52 | MTBE: Methyl Tertiary-Butyl Ether |
| 36 | DVPE: Vapour pressure | 53 | NO_x: Nitrogen oxides |
| 37 | E: Evaporated | 54 | R: Constant catalyst thermal reactivity |
| 38 | EC: EU Commission Regulation | 55 | RON: Research Octane Number |
| 39 | ECU: Engine Control Unit | 56 | SMPS: Scanning Mobility Particle Sizer |
| 40 | ETBE: Ethyl Tertiary-Butyl Ether | 57 | t_e: number of equivalent hours |
| 41 | EU: European Union | 58 | t_h: number of hours to complete a fixed |
| 42 | FTIR: Fourier Transform Infrared | 59 | distance |
| 43 | Spectroscopy | 60 | THC: Total Hydrocarbons |
| 44 | Fuel A: Additivated Fuel | 61 | T_v: pre-TWC temperature |
| 45 | Fuel B: Reference Fuel | 62 | TWC: Three Way Catalyst |
| 46 | GDI: Gasoline Direct Injection | | |

63

64 1. Introduction

65 A European Union (EU) long-term goal is the ambition of climate neutrality by 2050 (e.g. EU Energy
66 Roadmap 2050) which motivates decarbonisation of the transport sector [1]. Passenger cars are
67 forecasted to evolve towards battery electric vehicles (BEVs). However, a scenario where the utilisation

68 of ICE, as part of hybrid electric vehicles, in half of the vehicle fleet is predicted to lead to the same
69 reduction in greenhouse gases (GHG) as converting the whole fleet to BEVs [2]. It is expected that ICE,
70 and particularly efficient Gasoline Direct Injection (GDI) engines [3][4], to remain dominant [3] to
71 fulfil the global transport demand in the foreseeable future. The use of more efficient and cleaner fuels,
72 fuel blend components and fuel additives can contribute to the engine fuel economy improvement as
73 well as GHG and pollutant emissions reduction. Octane rating is a key fuel property to enable utilising
74 high compression ratio engines in order to improve performance and efficiency [5]. Octane improvers
75 (antiknock agents) are classified into fuel components (e.g. isoparaffins [6], olefins [7], alcohols [8],
76 ethers [9][10][11], esters [12], ketones [13], carbonates [14]) when the compound is generally present
77 in more than 2% vol., and fuel additives (e.g. anilines [15] [16], amines [17], N-nitrosamines [18],
78 phenols [19]). The use of fuel additives, being effective when used in lower amounts compared to fuel
79 components, is considered a practical and economic approach. Therefore, investigating combinations
80 of the most promising octane booster additives with high-octane components is recommended to obtain
81 high-octane gasoline that is technically, economically, and environmentally viable [20].

82 The first antiknock agents were tetraalkylated lead compounds, but both health and environmental
83 toxicity and the deteriorating impact on vehicle catalyst led to their usage prohibition [21][22]. Metallic
84 anti-knock agents, such as methylcyclopentadienyl manganese tricarbonyl and ferrocene can be used at
85 lower concentrations compared to lead compounds, but they tend to result in ash deposits in engine
86 components after their combustion. Aniline-like compounds (aromatic amines) are known by their
87 antiknock activity related to the abstraction of the amino hydrogen atom by reactive radical species and
88 being ash-less [23][24][25]; while their application has been often limited by their potential toxicity. A
89 recent study has classified anilines as one of the most promising fuel additives to be incorporated in
90 future gasoline formulations, accounting for their antiknock effectiveness, side effects on the engine,
91 possible effects on human health and the environment, and compatibility with existing infrastructure
92 [20]. N-methyl-p-anisidine, N',N'-diethyl-2-methyl-p-phenylenediamine and N-nitroso-diphenylamine
93 have been identified between more than 8 million aniline-like compounds considering reactivity as well
94 as environmental and toxicological risks [26]. It has been also recently demonstrated that the

95 incorporation of aniline as an octane enhancer to a modern gasoline fuel leads to an increase in vehicle
96 power, a decrease in the time required for acceleration, and a reduction in fuel consumption [27].

97 Catalytic components have been used in exhaust aftertreatment systems for around five decades to abate
98 vehicular emissions, and prevent them to be released to the atmosphere such as the Three Way Catalyst
99 (TWC) [28]. Maintaining the aftertreatment system's designed performance during its whole
100 operational life is a key to fulfil emissions regulations and reach the targeted positive impact on air
101 quality and climate change. In GDI engines the TWC durability in abating emissions depends on the
102 level and nature of engine-out species (including inhibitors/promoters [29][30], poisons, and
103 impurities), the exhaust gas/catalyst temperatures, the species' residence time within the aftertreatment
104 system, and the fluctuations in temperature, gas phase composition and flow rates. The TWC's
105 deactivation/ageing is linked to changes in the catalyst structure and state leading to the
106 deactivation/loss of active sites from the monolith surface and consequently to the deterioration of the
107 catalyst performance. A long-term exposure to high temperatures, high temperature gradients, and rich
108 and lean air-fuel ratio variations within the catalysts are the main factors leading to the substrate and
109 washcoat damages (thermal ageing) [33][34], and thus a loss in the catalytic activity. The major thermal
110 ageing mechanisms include thermal degradation (at around 800-900 °C) and sintering of the catalytic
111 active centres (at above 600 °C). Chemical ageing of the catalyst is generally caused by the
112 accumulation of non-desirable species, derived from fuels, lubricants and additives, on the catalytic
113 surfaces, and/or the suppression of its oxygen storage capacity. Sulphur in the fuel and/or lubricants has
114 been commonly identified as a non-desirable specie reducing the performance of the exhaust
115 aftertreatment components, e.g. NO_x adsorbers for lean GDI engines [35]. There are also other fuel
116 additives (e.g. lead and manganese), and wear inhibitor oil additives (e.g. Zinc dialkyldithiophosphates
117 [36]) considered as strong catalyst deactivators. However, the impact of advanced octane enhancement
118 additive compounds used in modern fuels on the performance and durability of the exhaust
119 aftertreatment components has not been extensively studied.

120 Legislators, researchers, and original equipment manufacturers have been working on developing
121 procedures to shorten the catalyst durability testing time by implementing alternative methods for

122 accelerated aging of catalysts [32]. The developed methodologies as well as most of the studies on
123 aftertreatment durability have been mainly focused on high temperature (thermal) ageing, as it is being
124 considered the dominant ageing mechanism. However, with the exhaust gas temperature being
125 progressively reduced over the years due to the development of the more efficient GDI engine
126 technology, it is of interest to separately investigate an accelerated chemical ageing procedure focused
127 on the effects of compounds that the catalyst is exposed to.

128 This work investigates the impact of using small concentrations of an advanced aniline derivative octane
129 enhancer additive in a modern gasoline fuel on the GDI engine combustion and emissions
130 characteristics, as well as the performance of a commercial TWC. A newly designed accelerated catalyst
131 ageing procedure with the main focus on chemical ageing is utilised to study the potential
132 synergies/interactions between the additivated high octane fuel and the TWC at different ageing stages.
133 Moreover, the transient response of the TWC to changes in its inlet gas coming from the engine during
134 the ageing procedure is examined. Additional objectives are to evaluate the size-resolved removal
135 efficiency of exhaust particle emissions by the TWC and the impact of the fuel on light-off
136 characteristics of the scaled-down TWC at the initial (fresh) and final stages (aged) of the ageing
137 procedure. All of the results are compared to those obtained when running on a baseline gasoline fuel.

138 **2. Material and Methods**

139 *2.1 Gasoline Direct Injection Engine*

140 The engine was a 2-L four-cylinder turbocharged GDI engine. The main engine specifications and a
141 schematic of the experimental setup are shown in Table 1 and Figure 1, respectively.

142 *2.2 Fuels and Catalysts*

143 The two fuels used in this study were provided by Repsol, both meeting the specifications for winter
144 gasoline EN-228. Fuel B (baseline) is a commercial type gasoline representing the grades distributed in
145 Spain (98 RON). Fuel A (additivated) is a modification of the 98 RON commercial gasoline (Fuel B)
146 by only adding an aniline derivative octane additive ($< 0.7\%$ v/v), with a target of 100 RON. It has to
147 be noted that the octane booster is added to a base fuel which already contained a high octane rating

148 component, i.e. ethyl tertiary-butyl ether (ETBE). The additive has a high efficiency to increase RON,
149 while it does not considerably change any other key fuel properties/characteristics as it can be seen in
150 Table 2. Two commercial full scale and two scaled-down TWCs were used for this study (Table 3).
151 Details about how these catalysts were tested are provided in sub-section 2.4.

152 *2.3 Instrumentation*

153 Engine speed and torque, critical fluid temperatures and data acquisition for a variety of analogue
154 signals were managed by the CADET control software from Sierra CP Engineering. The engine
155 manufacturer provided a development engine control unit (ECU), which enables access to the engine
156 calibration settings and sensors reading via Accurate technologies vision software. To acquire data from
157 the ECU, a controller area network hub was used. For this work the engine was operated with the
158 standard ECU calibration settings for both fuels (e.g. same injection, spark and valve timings).

159 Fuel consumption was measured with Rheonik RM015 Coriolis fuel flow meter ($\pm 0.12\%$ accuracy).
160 The fuel temperature was controlled by a Sierra CP Engineering fuel conditioning unit, and was
161 maintained at 28 °C for all the tests. An AVL piezo-electric pressure transducer and an AVL charge
162 amplifier were employed to measure in-cylinder pressure for fuel combustion analysis. In-cylinder
163 pressure values were referenced to each 0.5 crank angle degrees (CAD) using a crankshaft encoder. The
164 in-cylinder pressure was referenced to the intake manifold pressure at the intake bottom dead centre
165 using an absolute pressure transducer located in the intake runner close to the port entry. In-cylinder
166 pressure, real time indicated mean effective pressure (IMEP), coefficient of variation (COV) of IMEP,
167 peak pressure and position of peak pressure were acquired through in-house LabVIEW. Mass fraction
168 burnt was obtained using a custom Matlab post-processing script.

169 A 2030 MKS Fourier Transform Infrared Spectroscopy (FTIR) was used to measure the gaseous
170 exhaust species emitted from the engine (engine output or before the TWC, bTWC) as well as after the
171 TWC (aTWC) to calculate TWC conversion efficiency. The gaseous species included, but not limited
172 to, CO, NO_x, NH₃, CH₄ and total hydrocarbons (THCs). The gas sample was heated and maintained at
173 191 °C to prevent any water and HC condensation. A TSI Scanning Mobility Particle Sizer (SMPS)

174 was employed to measure particle size distributions before and after the TWC. The SMPS is composed
175 of a series 3080 electrostatic classifier, a 3081 Differential Mobility Analyser and a 3775 Condensation
176 Particle Counter. An ejector diluter was employed to dilute the exhaust gas by air before entering into
177 the SMPS. The dilution air temperature was kept constant at 150 °C in order to avoid hydrocarbon
178 condensation and nucleation.

179 *2.4 TWC ageing procedure*

180 The fuel effects on the TWC performance was evaluated under an accelerated ageing procedure. The
181 procedure was designed based on the TWC durability tests established by the EU Commission
182 Regulation (EC) No 692/2008 implementing and amending Regulation (EC) No 715/2007 of the
183 European Parliament and of the Council on type-approval of motor vehicles with respect to emissions
184 from light passenger and commercial vehicles [37][38]. The cycle is shown in Figure 2 and further
185 details can be found in Table 4.

186 The standard cycle estimates the number of equivalent hours (t_e) to carry out the accelerated ageing
187 tests based on the number of hours to complete a fixed distance, that in this case has been selected as
188 160,000 km (t_h); a pre-TWC temperature, in this case 500 °C (T_v); and a constant catalyst thermal
189 reactivity of 17,500 (R) as specified in the standard (see Equation 1). The number of hours was
190 calculated assuming a vehicle speed of 80 km/h. According to Equation 1, the duration of the ageing
191 test can be reduced by increasing the catalyst inlet temperature. However, as the aim of the present work
192 is to study the potential catalyst chemical ageing effect of the high octane rating additive, very high
193 catalyst inlet temperatures were avoided as this can result in catalyst thermal ageing, hindering the
194 effects of the fuel properties on TWC durability. A T_r pre-TWC temperature of 650 °C was chosen
195 resulting in a value of 50 h (t_e) of engine running to perform the accelerated ageing tests. Rapid pre-
196 catalyst rich and lean air/fuel changes by the combination of rich engine operation and external air
197 addition were implemented as suggested in the standard, Figure 2. The cycle was repeated for the total
198 duration of 50 hours.

$$t_e = t_n \exp \left[R \cdot \left(\frac{1}{T_r} - \frac{1}{T_v} \right) \right] \quad \text{Equation 1}$$

199 The engine condition selected for applying the standard cycle was 60 Nm, approximately 3.8 bar brake
 200 mean effective pressure, and 2100 rpm, at which engine operation stability and the pre-TWC target
 201 temperature were achieved. The internal exhaust gas recirculation technique was applied using the
 202 methods developed by the original equipment manufacturer. The engine intake air temperature was
 203 maintained at 45 °C while the coolant and oil temperatures were 95±0.5 °C and 99±2 °C, respectively
 204 for both fuels.

205 In order to achieve the target timings in the ageing procedure, an in-house Matlab script was developed
 206 and was linked to the ATI Vision to ensure that the automated sequence is repeated accurately (see
 207 Table 4). An Arduino microcontroller was used for accurate timing of the air injection in both main
 208 exhaust and reactor fitted in the furnace (Figure 1).

209 To carry out the tests for the two fuels, two full scale TWC were used (one per fuel) and fitted in a
 210 customised stainless steel casing (Figure 1). The exhaust gas temperatures before and after the TWCs
 211 were monitored using k-type thermocouples. The gaseous emissions measurements before and after the
 212 TWCs were recorded every hour during the ageing procedure. The conversion efficiency of various
 213 species in the TWC was assessed at steady state conditions every 5 hours of ageing.

214 The two scaled-down TWCs were used in parallel to investigate the ageing effects on the TWC light-
 215 off activity. They were placed in a stainless-steel reactor inside a furnace to control temperature and
 216 flow rate as shown in the experimental setup schematic (Figure 1). To mimic the operating conditions
 217 of the full scale TWCs and obtain comparable ageing effect for scaled-down cores, the gas temperatures
 218 at the inlet of the scaled-down TWCs and gas hourly space velocity (GHSV) for the cores were
 219 controlled during the tests. A small portion of engine-out exhaust gas was passed through the cores to
 220 maintain the GHSV at 40000 h⁻¹. The calculation of the GHSV is based on Equation 2:

$$\text{GHSV (h}^{-1}\text{)} = \frac{1}{\text{Contact time (h)}} = \frac{\text{Feed rate (m}^3\text{h}^{-1}\text{)}}{\text{Catalyst bed volume (m}^3\text{)}} \quad \text{Equation 2}$$

221 The light-off activity of the scaled-down TWC was investigated at the beginning (0 hour) and at the
222 end (50 hour) of the ageing process. The procedure to study the light-off activity was as follows: i) the
223 gas temperature at the inlet of the cores was initially maintained at 100°C, ii) once the engine reached
224 a steady-state condition, part of the exhaust stream was directed through the cores, iii) the gas
225 temperature was then increased with a ramp-up of 10 °C/min until 300 °C, at which CO and NO
226 conversion efficiencies were approximately 100%.

227 **3. Results and Discussion**

228 *3.1 Combustion analysis*

229 Combustion characteristics of the two fuels were studied through in-cylinder pressure and mass fraction
230 burnt traces (see Figure 3 left and right, respectively) at stoichiometric steady state engine condition
231 (2100 rpm, 60 Nm). There were no significant differences in the fuel combustion process under the
232 engine operating condition at which the ageing cycle was implemented. Therefore, it is believed that
233 any possible differences in emissions and TWC performance when using fuel A, compared to fuel B,
234 were not due to the combustion process, as their combustion characteristics were similar.

235 *3.2 Gaseous emissions: TWC performance at the steady-state stoichiometric condition*

236 Regulated gaseous emissions such as carbon monoxide (CO), nitrogen oxides (NO_x) and total
237 hydrocarbons (THC) have been analysed (Figure 4). These results are obtained by specifically operating
238 the engine at stoichiometric steady state engine operation (2100 rpm, 60 Nm) for the purpose of the
239 analysis. In addition, methane (CH₄) as one of the most challenging hydrocarbon species to be
240 catalytically oxidised [39][40], with a global warming potential of >20 times higher than CO₂ (over a
241 100 years period) [41], has been discussed. Stoichiometric engine-out emissions results, particularly for
242 CO and NO_x, showed small variations during the 50 hours of the ageing tests for each fuel, which
243 supports the repeatability of the experimental conditions (within 5-10%). Engine-out carbonaceous
244 emissions of CO, CH₄, and THC for fuel A (high octane rating fuel) were slightly lower (approximately
245 5%) than those for fuel B, while there were no significant differences in engine-out NO emissions.
246 These gaseous emissions results show a positive impact of the additive on the completion of the fuel

247 oxidation process. This positive impact is thought to be mainly induced by the chemical effect of the
248 additive as in-cylinder pressure and rate of heat released traces were not significantly different
249 compared to those of fuel B.

250 Gaseous emissions aTWC are shown in Figure 5. It has to be noted that the emissions levels for both
251 fuels remained at very low levels (under 80 ppm for CO and THC and below 10 ppm for NO emissions)
252 during the entire 50 hours duration of the ageing procedure. The results also show a slightly increasing
253 trend with time in aTWC THC gaseous emissions for fuel A, while there is not a clear trend in the case
254 of emissions for fuel B. The combination of the results shown in Figure 4 and Figure 5 evidence CO
255 and NO TWC conversion efficiencies close to 100% for both fuels during the whole accelerated catalyst
256 ageing procedure. There was a small decrease in catalyst conversion efficiency for THC for Fuel A and
257 for CH₄ emissions for both fuels with the ageing time of the catalyst. It is thought that this small decrease
258 in TWC conversion efficiency of unburnt HC is related to the TWC's oxygen storage capacity and not
259 to any additive-induced catalyst deactivation which would have resulted in much larger losses in TWC
260 activity. This is further explained in section 3.4 (TWC performance during the ageing cycle). In any
261 case, THC conversion efficiency was kept approximately 90% for both fuels after the representative
262 number of equivalent hours estimated from the standard cycle to study any potential chemical
263 deactivation. Therefore, there is no evidence of TWC deactivation during the developed accelerated
264 catalyst ageing procedure.

265 *3.3 Particle emissions: TWC performance at the steady-state stoichiometric condition*

266 Figure 6 illustrates the particle size distributions measured before and after the TWC at stoichiometric
267 steady state engine condition (2100 rpm, 60 Nm). The relative difference between them is also
268 calculated and denoted as particle reduction (removal) efficiency (Fuel A in blue and Fuel B in red
269 colour). Results show that particle concentration levels for fuels A and B were similar, while being
270 slightly lower (approximately 3% in terms of total particle concentration) for the case of the higher
271 octane rating fuel (Fuel A). This lower particle emissions is consistent with the slightly lower levels of
272 engine-out gaseous carbonaceous emissions discussed in section 3.2. The abatement of the number of
273 particles along the TWC was larger for small particle sizes (approximately 50% for particle sizes below

274 10nm), while it was in average approximately 10% across larger particle sizes. A similar trend was
275 observed for both fuels, though the TWC particle abatement efficiency for the additivated fuel was
276 slightly larger than for the baseline fuel. Similar TWC particle abatement efficiencies have been
277 reported [42], being attributed to the removal of some hydrocarbon species which can nucleate and form
278 small particles as well as some particle losses (mainly particle diffusion losses) along the TWCs,
279 especially noticeable for smaller particles [43].

280 Figure 7 shows the particle emissions measured before and after the TWC and their reduction efficiency
281 after applying the ageing procedure for both fuels (50 hours). Similar to the particle emissions levels at
282 the start of the tests and carbonaceous emission results, the engine-out particle emissions level for Fuel
283 A was slightly lower than the case of the base fuel. The effect of the aged TWC on particle levels was
284 similar to that of the TWC before applying the ageing procedure, as it can be seen from the same particle
285 reduction efficiencies in terms of pattern and values. Therefore, it can be concluded that the ageing
286 procedure has not affected the ability of the TWC in removing particles.

287 The comparison of the results shown in Figure 6 and Figure 7 indicates that particle removal efficiency
288 has not been affected by the ageing procedure. Particle removal efficiency over the TWC for small
289 particles (smaller than 10nm) was higher than that of larger particles for both fuels, which is a
290 characteristic of diffusion particle losses [44][45]. In addition, particle reduction efficiency for smaller
291 particles showed a larger dispersion than in the case of larger particles. This is believed to be due to the
292 lower particle concentrations and greater variability of nucleation mode particles (both bTWC and
293 aTWC).

294 *3.4 Gaseous emissions: TWC performance during the ageing cycle*

295 Gaseous emissions bTWC and aTWC were measured every hour during the catalyst ageing procedure
296 shown in Figure 2 (engine operation at stoichiometric 0-40 s, rich 41-45 s, rich with air injection in the
297 exhaust 46-55 s, and stoichiometric with air injection 56-60 s) for both fuels. This allows to assess the
298 fuel effects on emissions formation and catalyst performance under non-conventional (large variations
299 in lean and rich pre-catalyst conditions) and transient catalyst operating conditions at different stages
300 of the ageing procedure.

301 A representative example of bTWC and aTWC gaseous emissions corresponding to the catalyst ageing
302 cycle are shown in Figure 8 and Figure 9, respectively. In this particular case, emissions values were
303 recorded after 10 hours of the catalyst ageing procedure. During the cycle, at the engine stoichiometric
304 condition (from 0 to 40 s) engine-out CO, THC and NO emissions (Figure 8) were at similar levels to
305 those emitted at the steady-state engine condition used to evaluate the catalyst activity at every 5 hours
306 as shown in Figure 4. Engine-out CO and THC emissions for the higher octane rating fuel were slightly
307 lower than those for Fuel B, while there were no significant differences in engine-out NO emissions.
308 Moreover, similar to results in section 3.2, aTWC emissions were very low (Figure 9) for both fuels
309 indicating that the catalyst was working very efficiently at the stoichiometric condition (from 0 to 40
310 s).

311 As expected, when the GDI engine condition was changed to rich operation (from 41 to 45 s), engine-
312 out CO and THC emissions significantly increased (doubled up and 50% increase, respectively), while
313 engine-out NO and oxygen (not shown here) levels decreased (Figure 8). These changes in the pre-
314 TWC emissions produce an unbalanced level of reactants, which affects the TWC performance. The
315 aTWC CO and THC levels (Figure 9), significantly increased due to their inefficient oxidation in the
316 TWC as a result of the decreased levels of NO_x and oxygen. NO emissions remained at very low levels
317 (below 10 ppm, Figure 9) as there was an increased level of CO and THC that catalytically reduced
318 NO_x emissions.

319 Then, the air injection in the exhaust bTWC was activated (from 46 to 55 s). Engine-out emissions did
320 not change as the engine was kept under the same rich operation (Figure 8). The injection of air bTWC
321 led to a significant increase in aTWC NO emissions (Figure 9) due to the competition between NO and
322 oxygen to react with CO and THC within the TWC. Finally, the engine operation was changed to the
323 stoichiometric condition while maintaining the pre-TWC air injection, which significantly reduced
324 engine-out and aTWC CO and THC emissions.

325 Figure 10 shows the evolution of the conversion efficiency of gaseous emissions over the TWC during
326 the whole ageing experiments, when the engine was running under the stoichiometric condition with no
327 pre-TWC air injection. This engine and catalyst condition is comparable to the steady-state condition

328 analysed in section 3.2. However, in this case the data was taken from the transient ageing cycle (the
329 stoichiometric part) and thus is subject to the quick variations of the engine and catalyst conditions (e.g.
330 rich, lean and stoichiometric operation) which might affect the state of the TWC active sites. CO
331 (approximately 97%) and NO (approximately 99%) conversion efficiencies were very high for both
332 fuels for the entire duration of the ageing procedure. A slight reduction in THC, and CH₄, conversion
333 efficiency was observed for both fuels while the conversion efficiency for Fuel A (approximately 92%)
334 was generally lower than that for Fuel B (approximately 96%). The results and findings are comparable
335 to those obtained when the steady-state stoichiometric operating condition was evaluated (section 3.2),
336 indicating that the small reductions in conversion efficiency during the ageing procedure are not
337 significant to demonstrate any catalyst poisoning or deactivation.

338 TWC conversion efficiency has also been evaluated under the rich engine operation stage of the ageing
339 cycles (Figure 11). NO conversion efficiency was always 100% (not shown), while lower values of
340 conversion efficiency were recorded for CO and THC. There seemed to be a decrease in CO and THC
341 conversion efficiency along the ageing cycle performed on the same day (see Figure 11). It is thought
342 that the rich operation during the ageing cycle decreased the catalyst oxygen storage capacity and as a
343 result it reduced the catalyst performance under the rich condition at the later hours on the same day. In
344 the following day and at the start of the tests the catalyst conversion efficiency levels were partially
345 restored. The decrease in rich-phase catalyst performance was observed for both fuels reassuring that
346 such deterioration in TWC performance was not due to the fuels (additive package), but because of the
347 challenging catalyst conditions imposed by the ageing cycle.

348 *3.5 Light-off studies of the scaled-down TWCs*

349 Results presented in the previous sections were used to evaluate the catalyst performance at a
350 temperature (approximately 650 °C) beyond the catalyst light-off temperature. This section provides
351 the TWC performance results (in terms of CO conversion efficiency as a representative example) over
352 a wider and lower temperature range enabling to understand the fuel impact and TWC ageing effects
353 on the catalyst light-off performance. These conditions are relevant to the cold start engine operation.

354 Figure 12 shows similar CO TWC light-off activity for both fuels before the ageing procedure. These
355 results support that the differences in the emissions levels for Fuel A and B do not significantly affect
356 TWC light-off and conversion efficiency. Figure 12 also enables the comparison of the light-off
357 characteristics of the two TWCs (for fuel A and B) at the end of the accelerated ageing procedure.
358 Consistent with the full-scale catalyst study, no sign of deactivation was observed, given the similarity
359 in CO light-off temperatures for the two TWCs. These results support the non-significant catalyst
360 deterioration during the ageing procedure for both fuels as well as the absence of any potential TWC
361 poisoning induced by the additive.

362 **4. Conclusions**

363 An accelerated catalyst ageing method on a GDI engine has been designed aiming to investigate the
364 effects of an advanced aniline octane booster additive incorporated to a gasoline fuel on the TWC
365 performance. The ageing method has been designed with the focus to study TWC chemical ageing while
366 preventing thermal deactivation.

367 CO and NO TWC conversion efficiencies remained at ~99% over the duration of the accelerated ageing
368 procedure under steady-state and transient stoichiometric engine operation for both fuels. There was a
369 small decrease in the steady-state and transient stoichiometric TWC THC conversion efficiency;
370 however, such decrease was not significant to evidence TWC chemical deactivation as a result of using
371 the additivated fuel. The TWC light-off performance was also studied before and after the ageing
372 procedure. No sign of deactivation was observed supporting the non-significant catalyst performance
373 deterioration during the ageing procedure for both fuels.

374 This investigation demonstrates that fuels being designed to promote a more efficient/flexible GDI
375 engine operation can also enable the reduction of vehicle carbon footprint (CO₂ emissions) and tailpipe
376 pollutant emissions (through synergies with the aftertreatment) for cleaner road vehicles. The newly
377 designed high octane rating fuel, containing the aromatic amines, has demonstrated no detrimental
378 effects on the TWC performance over the accelerated catalyst ageing tests. This has been corroborated
379 at a large scale with the successful conclusion of commercial pilot phase of the fuel at three petrol
380 stations and its usage in various vehicles over the years with no reports of deteriorating effects.

381 **Acknowledgements**

382 This activity was part of the Project “Desarrollo de gasolina para motores eficientes” that has been
383 partially funded by Spanish CDTI (Centro de Desarrollo Tecnológico Industrial), identified as IDI-
384 20180217. Special appreciation goes to Dr. C. Hergueta, Mr. A. Wahbi, Mr Jack Garrod and Mr Kevan
385 Charlesworth for their contribution during engine experiments at the University of Birmingham as well
386 as to Dr. J. Aríztegui, Dr. M.D. Cardenas, Mr. D. Vanegas and Dr. C. Ruiz at Repsol for their
387 contribution on the conceptualisation of the work and fuel characterisation.

388

389 **References**

- 390 [1]. European Commission. A European Green Deal: Striving to be the First Climate-Neutral
391 Continent. 2019 Available online: [https://ec.europa.eu/info/strategy/priorities-2019-](https://ec.europa.eu/info/strategy/priorities-2019-2024/european-green-deal_en)
392 [2024/european-green-deal_en](https://ec.europa.eu/info/strategy/priorities-2019-2024/european-green-deal_en).
- 393 [2]. Concawe. Impact analysis of mass EV adoption and Low Carbon intensity fuel scenarios. 21
394 September 2018.
- 395 [3]. Duronio F, De Vita A, Montanaro A, Villante C. Gasoline direct injection engines – A review of
396 latest technologies and trends. Part 2. *Fuel* 2020; 265:116947.
- 397 [4]. Zhao F, Lai MC, Harrington DL. Automotive spark-ignited direct-injection gasoline engines.
398 *Prog Energy Combust Sci* 1999; 25:437–562.
- 399 [5]. Concawe. High-octane petrol (HOP) study: making gasoline relevant for the future of road
400 transport. Volume 28, Number 1, October 2019.
- 401 [6]. Dabelstein W, Reglitzky A, Schütze A, Reders K, Brunner A. In *Ullmann’s Encyclopedia of*
402 *Industrial Chemistry*; Wiley-VCH Verlag GmbH & Co. KGaA: Weinheim, Germany, 2016,
403 1–41, DOI: 10.1002/14356007.a16_719.pub3.
- 404 [7]. Magyar S, Hancsók J, Kalló D. Reactivity of Several Olefins in the HDS of full boiling point
405 range FCC gasoline over PtPd/USY. *Fuel Process Technol* 2008; 89(8):736–9.
- 406 [8]. Anderson JE, Kramer U, Mueller SA, Wallington TJ. Octane Numbers of Ethanol– and
407 Methanol–Gasoline Blends Estimated from Molar Concentrations. *Energy Fuels* 2010;
408 24:6576–85.
- 409 [9]. Cataluña R, Dalávia D, da Silva R, Menezes E, Venturi V, Wagner R. Acceleration tests using
410 gasolines formulated with di-TAE, TAEE and MTBE ethers. *Fuel* 2011; 90(3):992-996.
- 411 [10]. Nadim F, Zack P, Hoag GE, Liu SL. United States experience with gasoline additives. *Energy*
412 *Policy* 2001; 29(1):1-5.
- 413 [11]. Arteconi A, Mazzarini A, Di Nicola G. Emissions from ethers and organic carbonate fuel
414 additives: a review. *Water Air Soil Pollut* 2011; 221(1–4):405-23.
- 415 [12]. Jenkins RW, Munro M, Nash S, Chuck CJ. Potential renewable oxygenated biofuels for the
416 aviation and road transport sectors. *Fuel* 2013; 103:593–9.
- 417 [13]. Dahmen M, Marquardt W. Model-Based Design of Tailor-Made Biofuels. *Energy Fuels* 2016;
418 30:1109–34.

- 419 [14]. Chan J, Tsolakis A, Herreros JM, Kallis K, Hergueta Santos-Olmo C, Sittichompoo S, Bogarra
420 Macias M. Combustion, gaseous emissions and PM characteristics of Di-Methyl Carbonate
421 (DMC)-gasoline blend on Gasoline Direct Injection (GDI) engine, *Fuel* 2020; 263:116742.
- 422 [15]. Danilov AM. Fuel Additives: Evolution and Use in 1996-2000. *Chem Technol Fuels Oils* 2001;
423 37:444–55.
- 424 [16]. Brown JE, Markley FX, Shapiro H. Mechanism of Aromatic Amine Antiknock Action. *Ind Eng*
425 *Chem* 1955; 47(10):2141-6.
- 426 [17]. Skobelev VN, Yablokov VM, Serdyuk VV, Ashkinazi LA. Amines as antiknock compounds.
427 Phenomenological approach. *Russ J Appl Chem* 2007; 80:1225–34.
- 428 [18]. Akaribo B, Afotey B. Comparative analysis of selected octane enhancing fuel additives as a
429 substitute to methylcyclopentadienil Manganese Tricarbonyl (MMT). *Int J Energy Eng* 2017;
430 7:65–73.
- 431 [19]. Zhang P, Yee NW, Filip SV, Hetrick CE, Yang B, Green WH. Modeling study of the anti-knock
432 tendency of substituted phenols as additives: an application of the reaction mechanism generator
433 (RMG). *Phys Chem Chem Phys* 2018; 20:10637–49.
- 434 [20]. Badia JH, Ramírez E, Bringué R, Cunill F, Delgado J. New Octane Booster Molecules for
435 Modern Gasoline Composition. *Energy Fuels* 2021; 35:10949–97.
- 436 [21]. Benson SW. The mechanism of inhibition of knock by lead additives, a chain debranching
437 reaction. *J Phys Chem* 1988; 92:1531–3.
- 438 [22]. Seyferth D. The rise and fall of tetraethyllead. *Organometallics* 2003; 22:5154–78.
- 439 [23]. Ma H, Zhu Z, Wang B. Simple synthesis of N-methyl aniline over modified kaolin for octane
440 number improvement. *Energy Fuels* 2008; 22:2157–9.
- 441 [24]. Cullis CF, Holwill JM, Pollard RT. The influence of amines on the combustion of nheptane.
442 *Symp Combust* 1971; 13:195–203.
- 443 [25]. Boot MD, Tian M, Hensen EJM, Mani Sarathy S. Impact of fuel molecular structure on
444 autoignition behavior - Design rules for future high performance gasolines. *Prog Energy Combust*
445 *Sci* 2017; 60:1–25.
- 446 [26]. Viayna A, Ghashghaei O, Vílchez D, Estarellas C, López M, Gómez-Catalán J, Lavilla R,
447 Delgado J, Javier Luque F. Holistic approach to anti-knock agents: A high-throughput screening
448 of aniline-like compounds. *Fuel* 2021; 305:121518.
- 449 [27]. Rodriguez-Fernandez J, Ramos A, Barba J, Cardenas MD, Delgado J. Improving Fuel Economy
450 and Engine Performance through Gasoline Fuel Octane Rating. *Energies* 2020; 13(13):3499.

- 451 [28]. Harrison B, Cooper BJ, Wilkins AJJ. Control of Nitrogen Oxide Emissions from Automobile
452 Engines. The development of Rhodium/Platinum three way catalyst systems. *Metals Rev* 1981;
453 25(1):14-22.
- 454 [29]. Lefort I, Herreros JM, Tsolakis A. Reduction of Low Temperature Engine Pollutants by
455 understanding the Exhaust Species Interactions in a Diesel Oxidation Catalyst. *Environ Sci*
456 *Technol* 2014; 48(4):2361-7.
- 457 [30]. Fayad MA, Fernández-Rodríguez D, Herreros JM, Martos FJ, Lapuerta M, Tsolakis A.
458 Interactions Between Aftertreatment Systems Architecture and Combustion of Oxygenated Fuels
459 for Improved Low Temperature Catalysts Activity. *Fuel* 2018; 229:189-97.
- 460 [31]. Cooper BJ. Durability of Platinum-Containing Automotive Exhaust Control Catalysts.
461 Improvements in resistance to thermal degradation. *Platinum Metals Rev* 1983; 27(4):146-55.
- 462 [32]. Ignatov D, Küpper C, Pischinger S, Bahn M, Betton W, Rütten O, Weinowski R. Catalyst Ageing
463 Method for Future Emissions Standard Requirements. SAE Technical Paper 2010-01-1272.
- 464 [33]. Rohart E, Larcher O, Hédouin C, Allain M, Macaudière P. Innovative Materials with High
465 Stability, High OSC, and Low Light-Off for Low PGM Technology. SAE Technical Paper 2004-
466 01-1274.
- 467 [34]. Dagobert, P. *Automobiles and Pollution*, SAE, Warrendale, PA, USA, 1995, ISBN 1-56091-563-
468 3.
- 469 [35]. Fridell E, Skoglundh M. Model Studies of Sulphur Deactivation of NO_x Storage Catalysts. SAE
470 Technical Paper 2004-01-0080.
- 471 [36]. Lafyatis DS, Petrow R, Bennett C. The Effects of Oil-derived Poisons on Three-Way Catalyst.
472 Performance. SAE Technical Paper 2002-01-1093.
- 473 [37]. European Commission, Regulation (EC) No 692/2008. Official Journal of the European Union,
474 rev. 18th of July 2008.
- 475 [38]. Galassi MC, Martini G. Durability Demonstration Procedures of Emission Control Devices for
476 Euro 6 Vehicles. EUR 26435. Luxembourg (Luxembourg): Publications Office of the European
477 Union; 2014. JRC87070.
- 478 [39]. Diehl F, Barbier Jr J, Duprez D, Guibard I, Mabilon G. Catalytic oxidation of heavy hydrocarbons
479 over Pt/Al₂O₃. Influence of the structure of the molecule on its reactivity. *Appl Catal B-Environ*
480 2010; 95:217–27.
- 481 [40]. Herreros JM, Gill SS, Lefort I, Tsolakis A, Millington P, Moss E. Enhancing the low temperature
482 oxidation performance over a Pt and a Pt-Pd diesel oxidation catalyst. *Appl Catal B-Environ*
483 2014; 147:835–41.

- 484 [41]. US EPA. Atmospheric Lifetime and Global Warming Potential Defined/US EPA. 2018. [online]
485 Available at: [https://www.epa.gov/climateleadership/atmospheric-lifetime-and-global-warming-](https://www.epa.gov/climateleadership/atmospheric-lifetime-and-global-warming-potential-defined)
486 [potential-defined](https://www.epa.gov/climateleadership/atmospheric-lifetime-and-global-warming-potential-defined).
- 487 [42]. Bogarra M, Herreros JM, Tsolakis A, York APE, Millington P. Study of particulate matter and
488 gaseous emissions in gasoline direct injection engine using on-board exhaust gas fuel reforming.
489 Appl Energy 2016; 180:245-55.
- 490 [43]. Bogarra M, Herreros JM, Hergueta C, Tsolakis A. Influence of three-way catalyst on gaseous
491 and particulate matter emissions during gasoline direct injection engine cold-start. Johnson
492 Matthey Technol Rev 2017; 61(4):329-41.
- 493 [44]. Hinds CW. Aerosol Technology: Properties, Behavior, and Measurement of Airborne Particles.
494 Wiley 2nd Edition, 1999.
- 495 [45]. Von der Weiden SL, Drewnick F, Borrmann S. Particle Loss Calculator – a new software tool
496 for the assessment of the performance of aerosol inlet systems. Atmos Meas Tech 2009; 2:479-
497 94.

498 **List of Figures**

499 **Figure 1.** Schematic of the experimental setup

500 **Figure 2.** Standard Bench Cycle

501 **Figure 3.** Engine combustion in-cylinder pressure and mass fraction burnt of fuel A (additivated) and
502 fuel B (baseline)

503 **Figure 4.** Engine-out (bTWC) emissions under the stoichiometric engine condition at every 5 hours

504 **Figure 5.** After TWC (aTWC) emissions under the stoichiometric engine condition at every 5 hours

505 **Figure 6.** Particle emissions under the stoichiometric engine operation at 0 hours, fuel A (additivated)
506 on the left and fuel B (baseline) on the right

507 **Figure 7.** Particle emissions under the stoichiometric engine operation after the TWC ageing procedure,
508 fuel A (additivated) on the left and fuel B (baseline) on the right

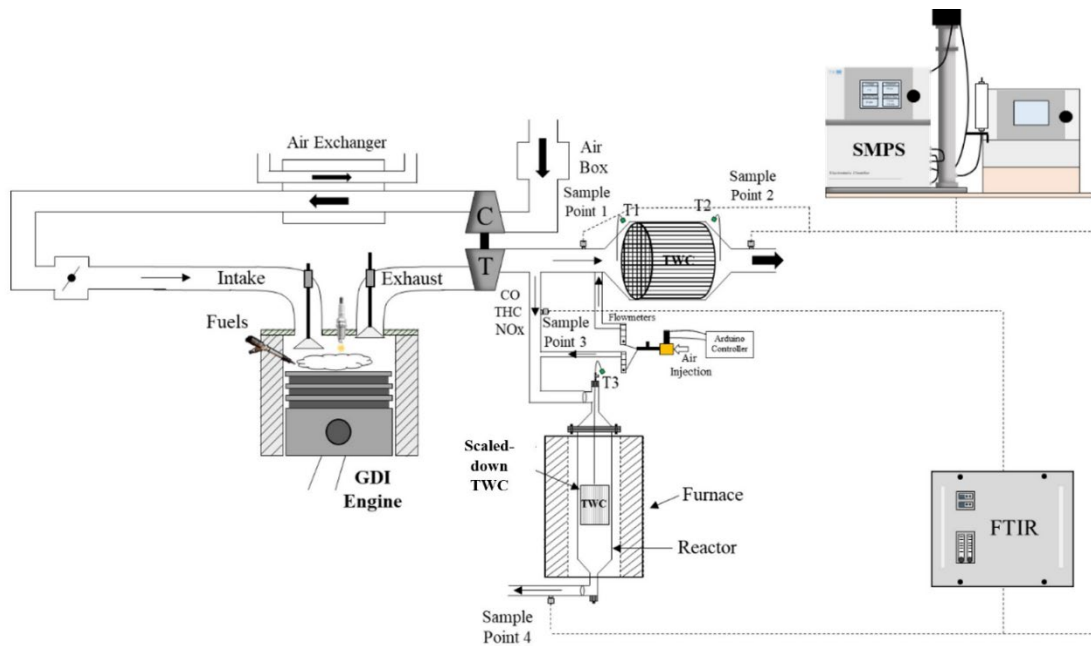
509 **Figure 8.** Engine-out gaseous emissions before TWC (bTWC) for Fuel A (top figure) and Fuel B
510 (bottom figure) during the cycle

511 **Figure 9.** Gaseous emissions after TWC (aTWC) for Fuel A (top figure) and Fuel B (bottom figure)
512 during the cycle

513 **Figure 10.** TWC conversion efficiency for gaseous emissions at the stoichiometric engine condition
514 during the procedure at every hour

515 **Figure 11.** TWC conversion efficiency for gaseous emissions at the rich engine condition during the
516 cycle at every hour

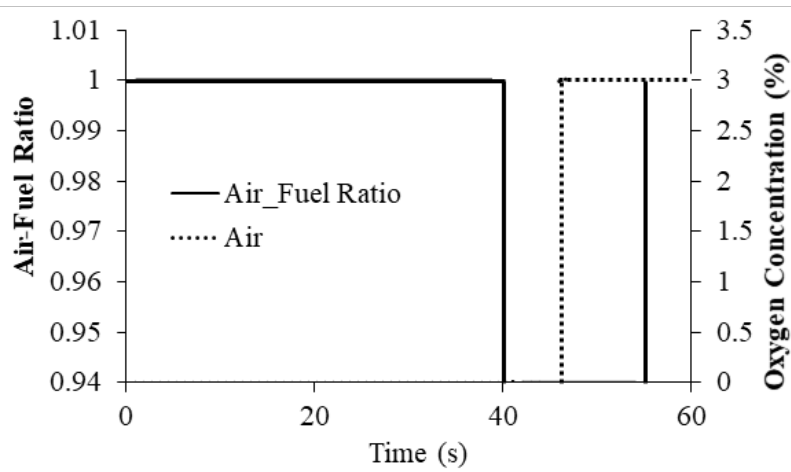
517 **Figure 12.** Scaled-down TWCs light-off before and after the ageing procedure



518

519

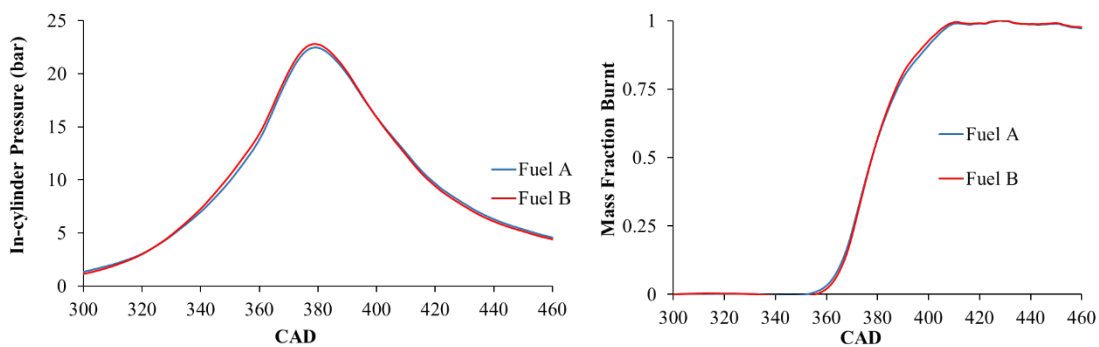
Figure 1



520

521

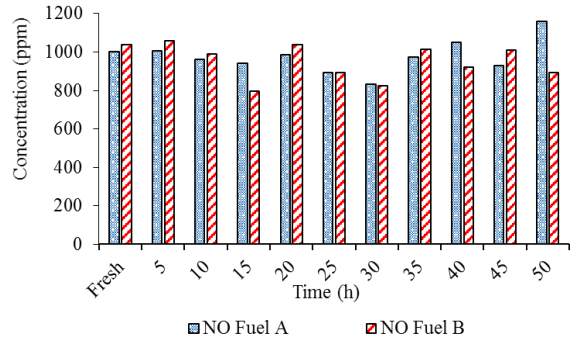
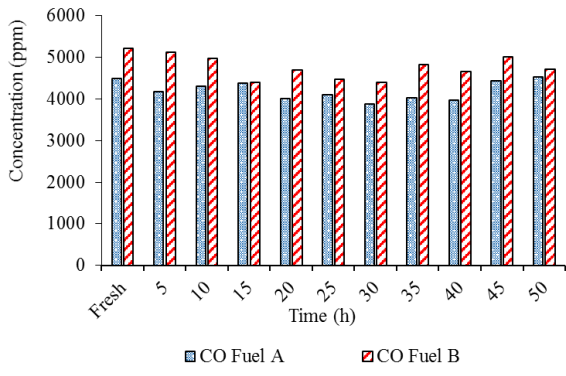
Figure 2



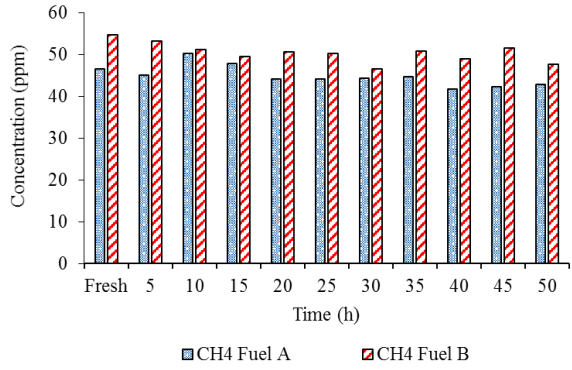
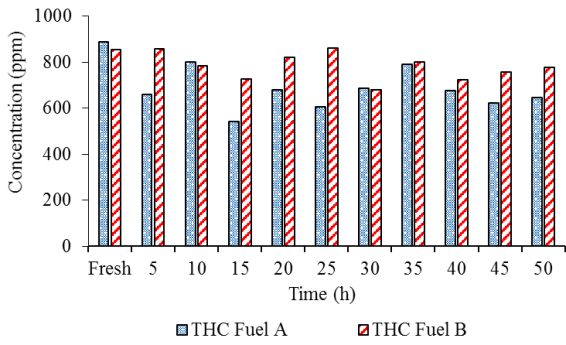
522

523

Figure 3



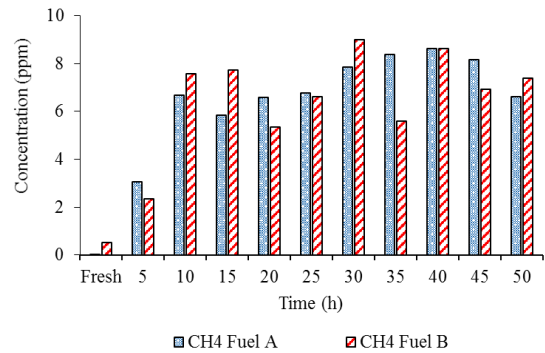
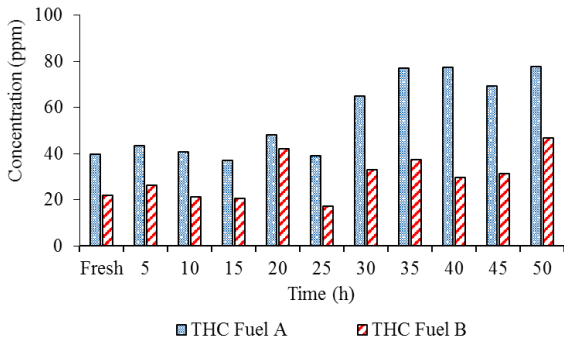
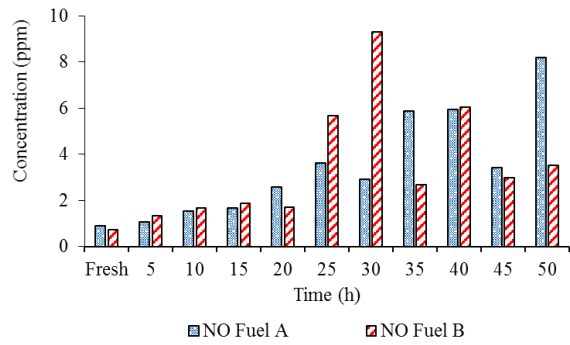
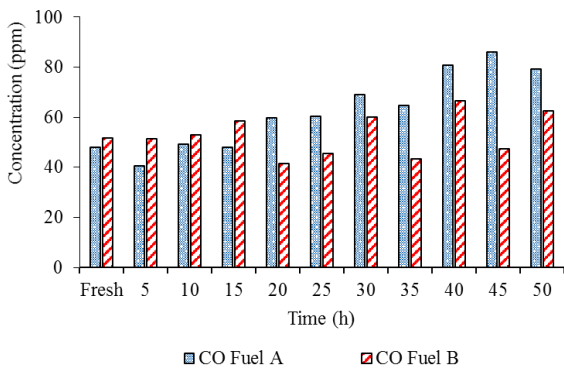
524



525

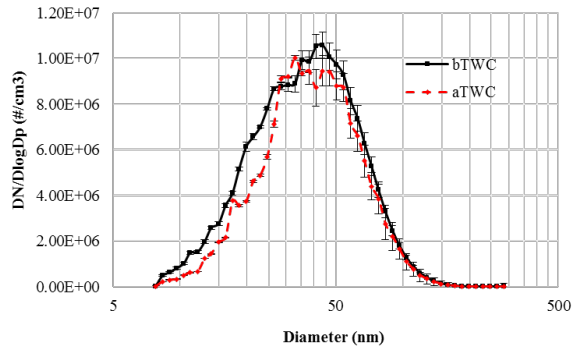
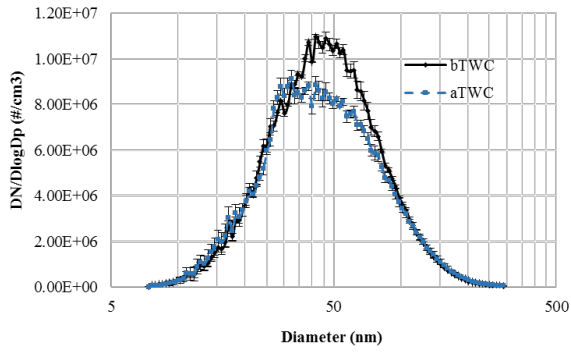
526

Figure 4

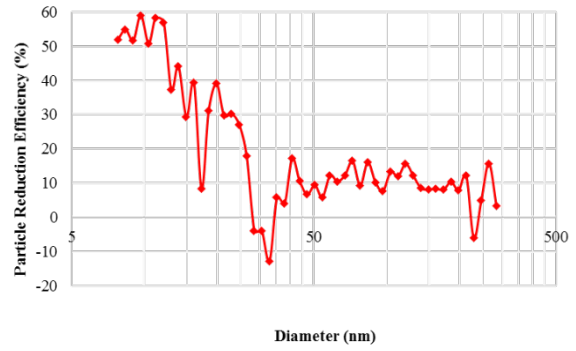
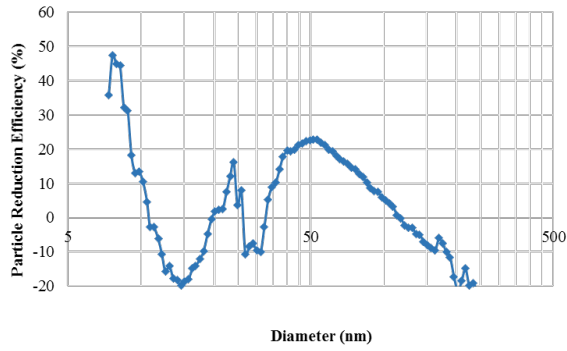


527

Figure 5



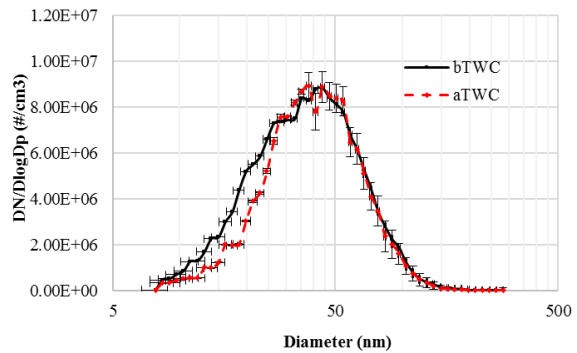
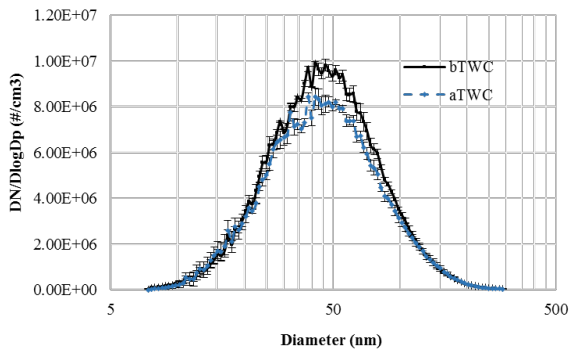
528



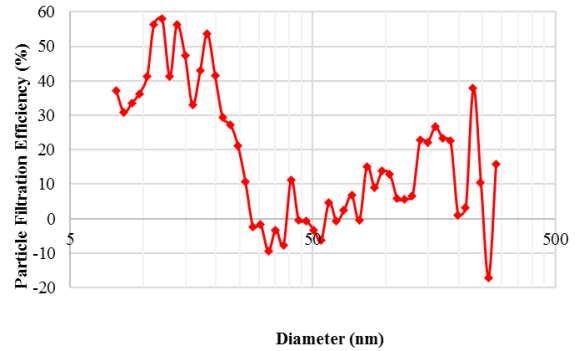
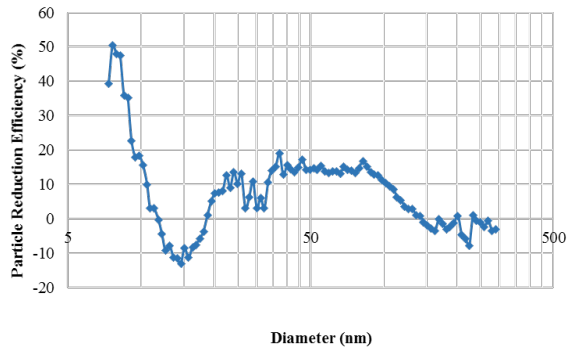
529

530

Figure 6



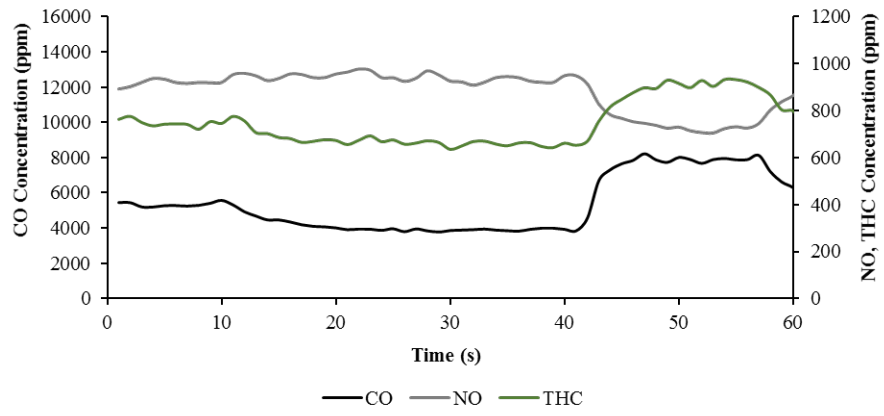
531



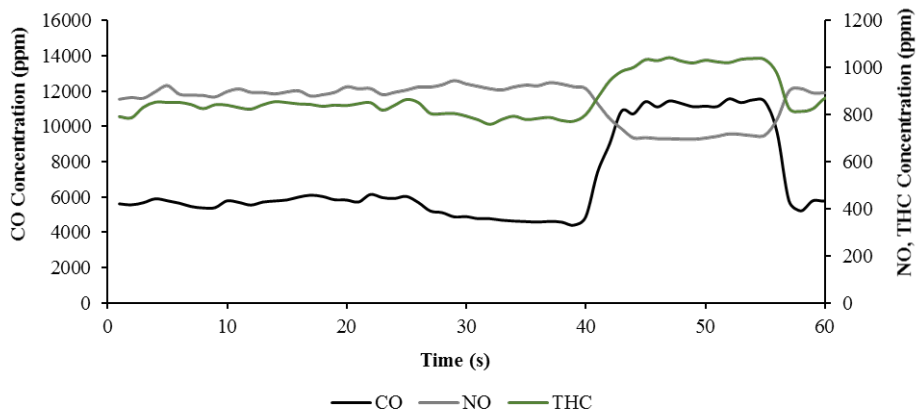
532

533

Figure 7



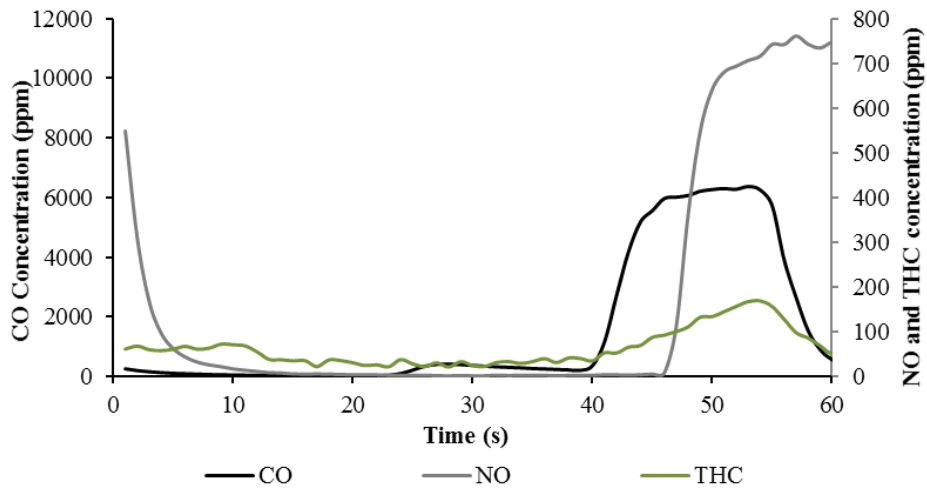
534



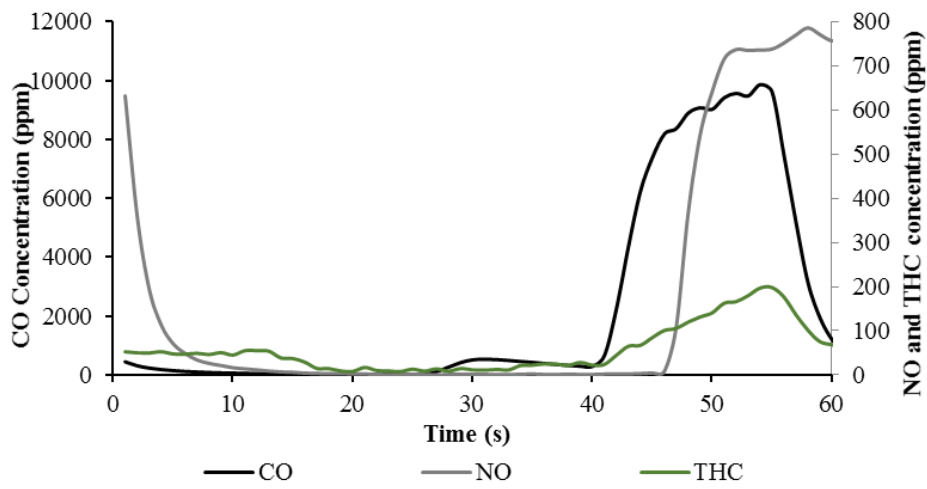
535

536

Figure 8



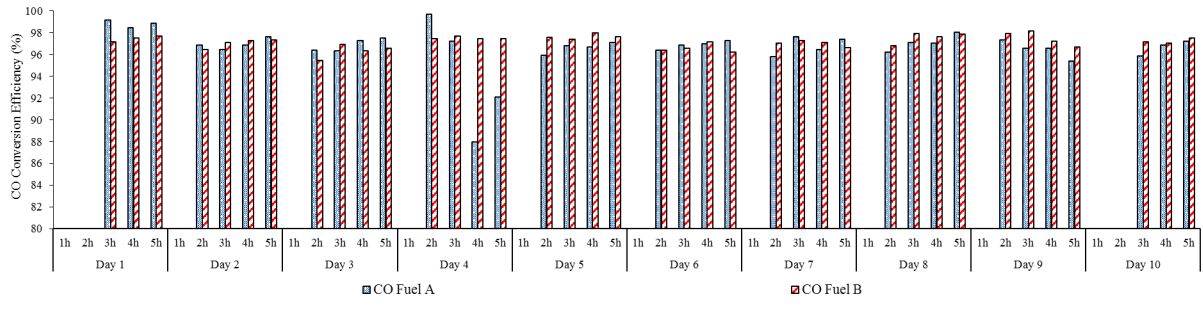
537



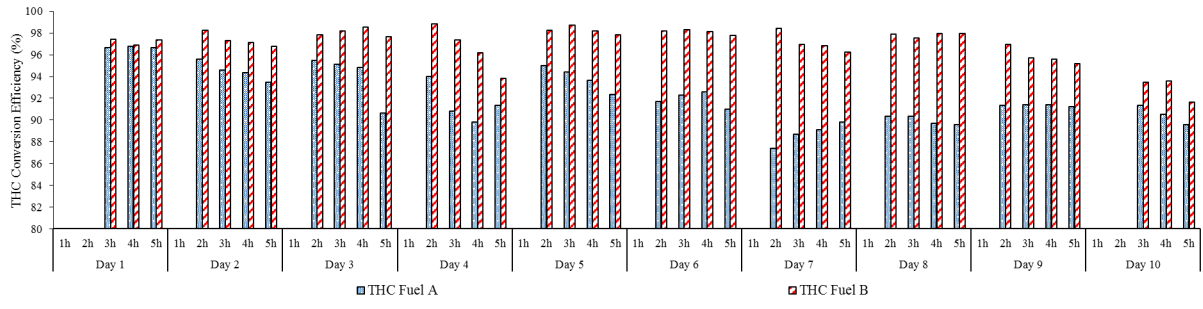
538

539

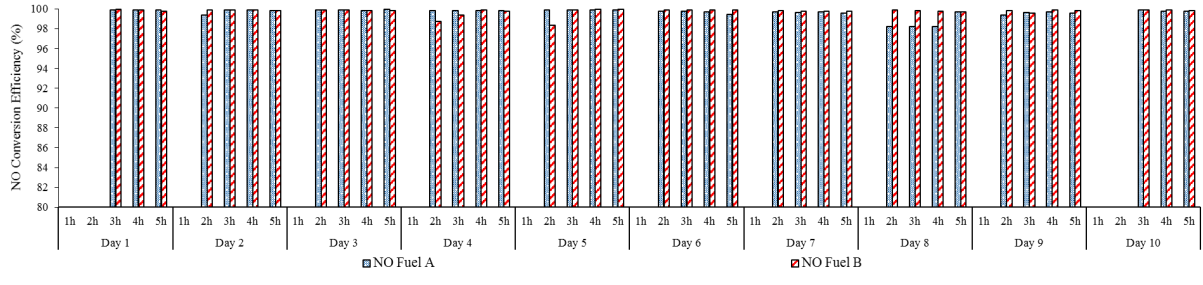
Figure 9



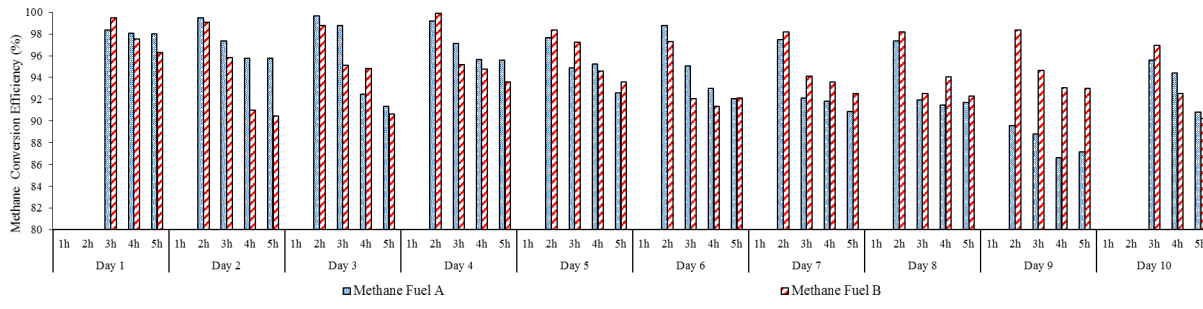
540



541



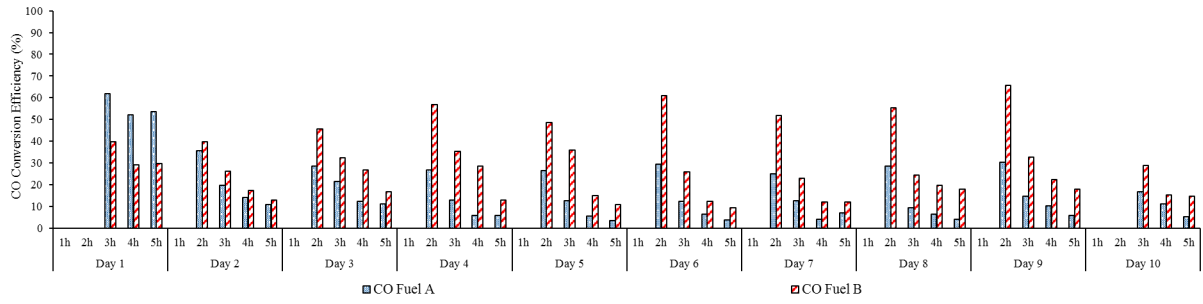
542



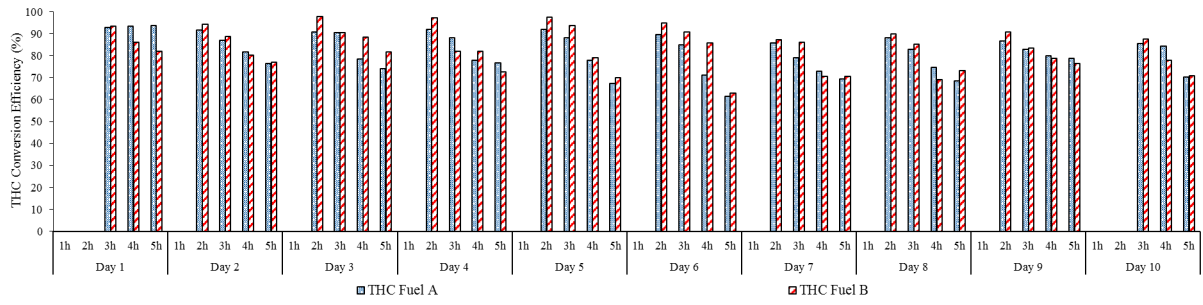
543

544

Figure 10



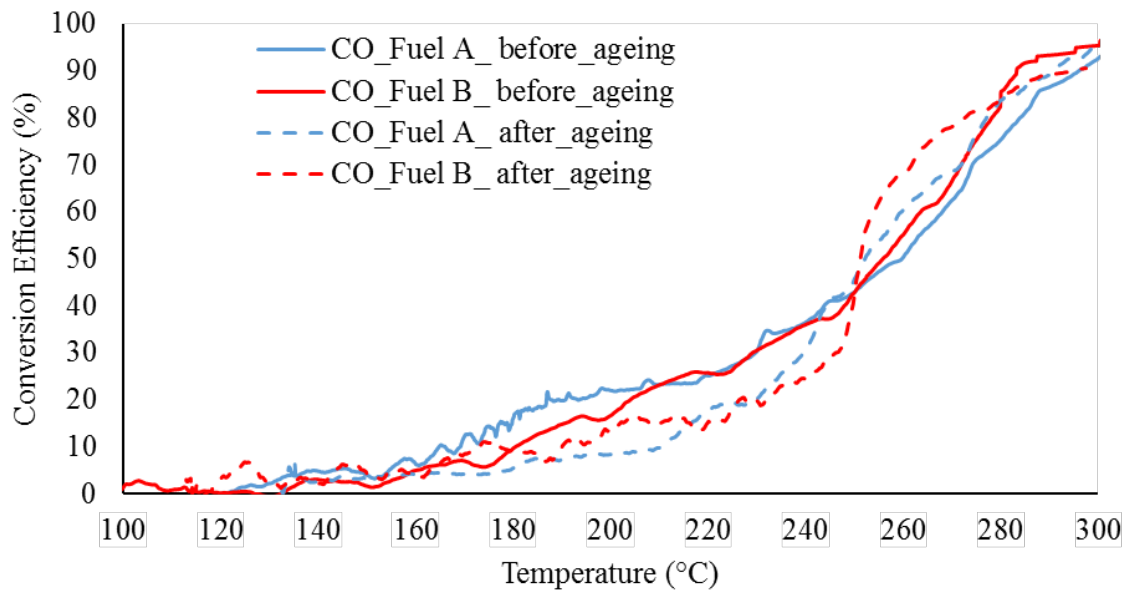
545



546

547

Figure 11



548

549

Figure 12

550	List of Tables
551	Table 1. Engine Specifications
552	Table 2. Fuel properties
553	Table 3. General catalyst characteristics
554	Table 4. Ageing stages of Standard Bench Cycle
555	

556

Table 1

Specification	Value
Compression Ratio	10:1
Bore × Stroke	87.5 × 83.1 mm
Turbocharger	Borg Warner K03
Rated Power	149 kW at 6000 rpm
Rated Torque	300 Nm At 1750-4500 rpm
Engine Management	Bosch Me17

557

558

559

560

561

Table 2

Property	Standard	Units	Min	Max	Fuel B Base	Fuel A Additivated
Research Octane Number (RON)	ASTM D 2699-18a	-	98.0	-	98.1	99.5
Motor Octane Number (MON)	ASTM D 2700-18a	-	85.0	-	87.8	87.8
Density @ 15 °C	ASTM D 4052-18	kg/m ³	720	775	734.9	736.8
Vapour pressure (DVPE)	ASTM D 5191-15	kPa	50	80	71.9	71.9
Distillation curve	ASTM D 86-17					
Evaporated @ 70 °C (E70)		% v/v	22	56	32.0	33.2
Evaporated @ 100 °C (E100)		% v/v	46	74	55.9	57.2
Evaporated @ 150 °C (E150)		% v/v	75	-	82.6	83.8
Final Boiling Point		°C	-	210	191	198
Residuals		% v/v	-	2	1.1	1.0
Sulphur	ASTM D 4294-16e1	mg/kg	-	10	< 10	< 10
Lead	UNE EN 237:2005	mg/l	-	5.0	< 0.003	< 0.003
HC composition	UNE EN ISO 22854:2016					
Olefins		% v/v	-	18.0	11.4	11.5
Aromatics		% v/v	-	35.0	24.5	24.7
Benzene		% v/v	-	1.0	0.68	0.69
Oxygen		% m/m	-	2.7	2.32	2.38
Methanol	% v/v	-	3	< 0.01	< 0.01	
Ethanol	% v/v	-	5	0.65	0.66	
Isopropyl alcohol		% v/v	Limited by maximum oxygen content		0.13	0.17
Tert-butyl alcohol		% v/v	-		< 0.01	< 0.01
Iso-butyl alcohol		% v/v	-		< 0.01	< 0.01
MTBE		% v/v	-		< 0.1	< 0.1
ETBE		% v/v	-		13.2	13.5
Ether compounds longer than C5					14.2	14.5
Other oxygenated compounds		% v/v	-		< 0.1	< 0.1

562

Table 3

TWC Characteristics		
Monolith	Substrate (cpsi/mil)	Dimensions (inch)
Full scale TWC	400/4.3	ϕ 4.66 \times 4.5
Scaled-down TWC	400/4.3	ϕ 1 \times 4.5

563

Table 5

Time (seconds)	Engine Air/Fuel Ratio	Secondary oxygen (air) injection
1-40	Stoichiometric	None
41-45	Rich with lambda = 0.94	None
46-55	Rich with lambda = 0.94	3% (\pm 1%)
56-60	Stoichiometric	3% (\pm 1%)

564